POLITECNICO DI TORINO
Repository ISTITUZIONALE

Numerical Modeling of Dapped-End Beams Subjected to Corrosion and Retrofitting Interventions

Original
Numerical Modeling of Dapped-End Beams Subjected to Corrosion and Retrofitting Interventions / Di Benedetto, M., Di Trapani, F., Sberna, A.P., Villar, S., Ferrara, M., Bertagnoli, G.. - 638:(2025), pp. 111-121. (Eurasian OpenSees Days 2024 Beijing (China) July 24–25, 2024) [10.1007/978-3-031-90690-9_10].

Availability:
This version is available at: 11583/3002229 since: 2025-08-25T07:16:54Z

Publisher:
Springer

Published
DOI:10.1007/978-3-031-90690-9_10

Terms of use:

This article is made available under terms and conditions as specified in the corresponding bibliographic description in the repository

Publisher copyright
Springer postprint/Author's Accepted Manuscript (book chapters)

This is a post-peer-review, pre-copyedit version of a book chapter published in Proceedings of the 2024 Eurasian OpenSees Days. The final authenticated version is available online at: http://dx.doi.org/10.1007/978-3-031-90690-9_10

(Article begins on next page)

26 November 2026

Numerical modeling of dapped-end beams subjected to corrosion and retrofitting interventions

Marilisa Di Benedetto[1], Fabio Di Trapani[1], Antonio Pio Sberna[1], Sofia Villar[1], Mario Ferrara[1], Gabriele Bertagnoli[1].

[1]Dipartimento di Ingegneria Strutturale, Edile e Geotecnica, Politecnico di Torino, Italy
marilisa.dibenedetto@polito.it

Abstract. This study concerns refined numerical modeling of dapped-end beams subjected to corrosion and the assessment of the performance of an external steel retrofitting system. Widely used in infrastructure heritage, dapped-end beams face several challenges due to the complex stress flows in the discontinuous zones caused by the abrupt change in section depth. To gain a better insight into the impact of local stress transfer and overall performance, extensive numerical investigations are essential. In this study refined 3D solid models are built to complement previous experimental tests on a steel retrofitting system for corrosion-damaged half-joints using the STKO software platform for OpenSees. The results from the experimental campaign are replicated numerically following a process of calibration of material parameters. Then, additional numerical simulations are carried out to examine the structural response of the retrofitted half-joint in different configurations not previously assessed in the reference experimental campaign. An improvement of the steel retrofitting system is finally proposed and numerically simulated. The results aim to provide insights into the efficiency and performance of retrofitted damaged half-joints, highlighting the capability of numerical models to complement experimental tests and improve the understanding of structural behavior, and strengthening strategies.

Keywords: Dapped-end beams, Half-joints, Bridges, Concrete, Retrofitting, OpenSees, STKO.

1 Introduction

Reinforced concrete infrastructures have shown significant deterioration due to aging, insufficient maintenance, and design flaws [1]. Issues such as carbonation, reinforcement corrosion, and cover spalling severely reduce load-bearing capacity in reinforced concrete bridges, requiring strengthening and retrofitting systems.

Dapped-end beams, also known as half-joint beams, are a notable example of structures often subjected to degradation especially because of corrosion of reinforcement (Fig.1). These structural elements, widely used from the 1960s to the 1980s for their design simplicity and settlement insensitivity, have shown early degradation and brittle failures [2, 3]. Several studies have evaluated the performance of dapped-end beams under both undamaged and damaged conditions, employing Strut-and-Tie models (STMs) [4]. Recent research has focused on experimental and numerical investigation of the impacts of reinforcement corrosion and retrofitting solutions for structural deficiencies [5-10].



Fig. 1. Degradation of dapped-end beam bridges caused by steel reinforcement corrosion.

Two common strengthening techniques are Fiber Reinforced Polymers (FRP/CFRP) and external prestressing systems. While FRP/CFRP systems can increase load-bearing capacity by 10–80%, their effectiveness depends on geometric details, reinforcement layout, and fiber orientation [11–14]. On the other hand, external prestressing provides higher performance even if it is more difficult to install [15]. Among recent innovations, precast strain-hardening cementitious composites (P-SHCC) have demonstrated remarkable improvements, achieving up to a 90% performance increment [16].

However, most research on dapped-end beams focused on rectangular cross-sections, with limited attention to T-shaped sections, especially under severe damage conditions. To close this gap, an experimental campaign [17] was conducted to evaluate an innovative steel retrofitting technique consisting of L-shaped plates and transverse prestressing to transfer shear forces through friction, thereby avoiding damaged concrete sections. Tests carried out on scaled T-beams with two reinforcement layouts revealed significant improvements in resistance but also highlighted issues with the flange-web interface [17]. Based on this experimental campaign, the current study incorporates advanced numerical modeling using refined 3D solid models developed with the STKO software platform for OpenSees [18-19]. Numerical simulations replicate experimental results through material calibration and extend the analysis to explore structural behavior under configurations not previously tested. Based on the numerical results, an improved retrofitting system is proposed and numerically validated.

This study contributes to the understanding of the retrofitting system's efficiency, highlighting the synergy between experimental and numerical approaches, which

may be useful for retrofitting corrosion-damaged half-joints and enhancing the durability and safety of aging infrastructures.

2 Reference experimental campaign

The experimental campaign [17] involved two T-shaped dapped-end beam specimens scaled to 1:3 of typical bridge girders. Each specimen was 75 cm deep, with a flange width of 80 cm and an overall length of 490 cm, designed to replicate a longitudinal bridge beam connected rigidly to a pier [17]. The beams were cast in two stages: the flanges and webs were cast at different times to simulate the installation of half-joints in real structures. Both specimens had identical geometries but differed in their reinforcement layouts. One beam featured orthogonal reinforcement in the dapped-end region, while the other used inclined reinforcement, as illustrated in Fig. 2.

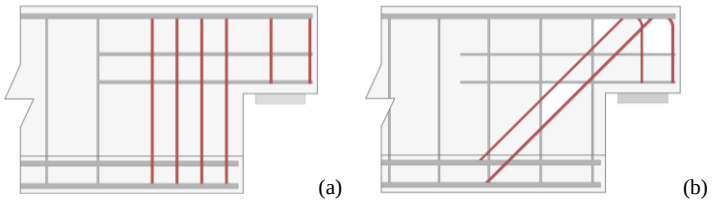


Fig. 2. Reinforcement layout of the dapped-end beam specimens: (a) Beam A; (b) Beam B.

One half-joint of each specimen was designed with reduced reinforcement to simulate the damage due to steel bar corrosion (damaged zone). The other half-joint was designed using the Strut-and-Tie (S&T) method and arranged with full reinforcement as a reference for comparison (undamaged zone). The damaged ends of both specimens (beams A and B) were strengthened using a steel jacketing system consisting of L-shaped steel plates with transverse prestressing bolts, as reported in Fig. 3. The system was designed to restore the load-bearing capacity by transferring shear forces through friction between the plates and the concrete web, bypassing weakened concrete areas. For the sake of brevity, additional details can be found in Bertagnoli et al. [17], which presents the design of the specimens and the retrofitting system.

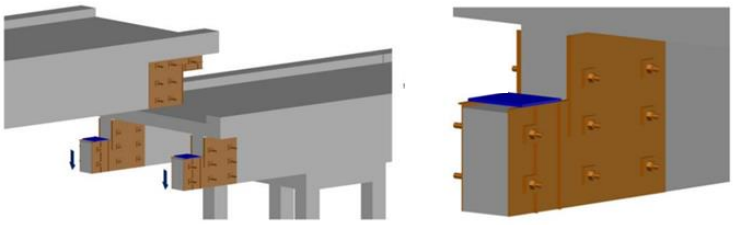


Fig. 3. Steel-jacketing system designed by Bertagnoli et al. [17].

The specimens were tested with vertical loads applied at midspan through a hydraulic jack. Both ends of the beams were supported at the half-joints to replicate the boundary conditions of actual bridge beams. The test setup included two static schemes: in the first configuration, both half-joints were loaded simultaneously, while the second configuration focused on the failure of the undamaged half-joint. Fig. 4 illustrates the static schemes adopted for the experimental tests of the two beams: static scheme 1 (SS1) and static scheme 2 (SS2).

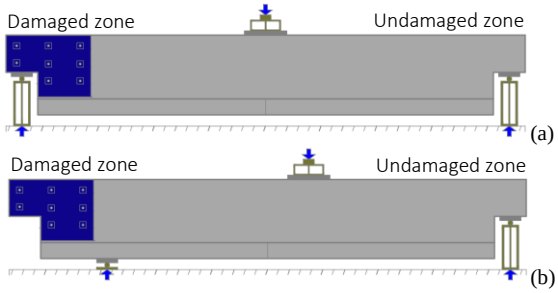


Fig. 4. Static schemes adopted for the experimental program: (a) Static scheme 1 (SS1); (b) Static scheme 2 (SS2).

Preliminary results of the experimental campaign are provided in [17].

3 Refined FE modeling of the dapped-end beams

3.1 Modeling strategy with OpenSees / STKO

A refined numerical modeling approach was employed to simulate the nonlinear behavior of dapped-end beams by replicating the experimental campaign and extending the analyses to other configurations. The models were developed within the STKO graphical interface for OpenSees [18-19], by using advanced damage mechanics and 3D finite element modeling to consider the anisotropic response of concrete and its interaction with the retrofitting system. A scheme of the model is illustrated in Fig. 5.

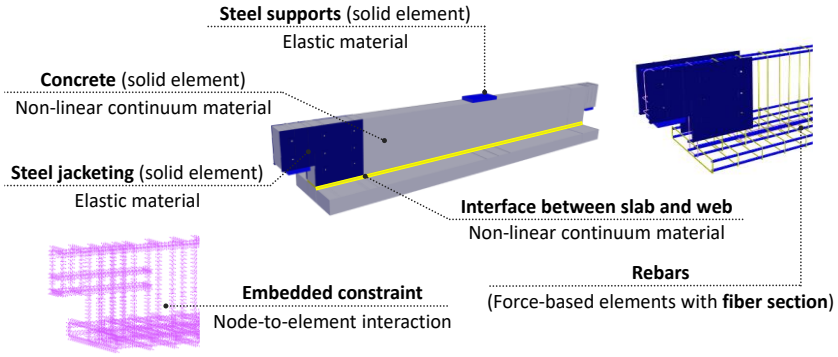


Fig. 5. Refined FE model of the dapped-end beam in OpenSees / STKO.

Concrete behavior was defined using the *ASDConcrete3D* constitutive model [20-21], which applies distinct damage indices for tension (d^+) and compression (d^-) to compute the update of the effective stress tensor $\boldsymbol{\sigma}$ at each step of the analysis. The latter is evaluated as follows:

$$\boldsymbol{\sigma} = (1-d^+)\bar{\boldsymbol{\sigma}}^+ + (1-d^-)\bar{\boldsymbol{\sigma}}^- \tag{1}$$

where $\bar{\boldsymbol{\sigma}}^+$ and $\bar{\boldsymbol{\sigma}}^-$ are the positive and negative components of the effective stress tensors, respectively.

Steel reinforcement was modeled as 1D fiber-section *force-based beam-column* elements with a *Hysotropic* material. The rebars are seamlessly connected to the concrete beam using *ASDEmbedded-node* elements to simulate perfect bonding. The steel jacketing retrofitting system, modeled with 3D solid elements, was linked to the beam through *Zero-Length-Implex-Contact* elements simulating frictional and shear interactions using a Coulomb friction law [22-23].

3.2 Analyses and model validation

The boundary conditions of the model replicated the experimental setup. Incremental vertical loads were added to consider gravity, followed by monotonic displacement to simulate failure. A quadratic mesh with an average element size of 30 mm was optimized for computational efficiency and accuracy. The analysis outputs included load-displacement curves (Fig. 6) and crack propagation patterns (Fig. 7), which provided detailed insights into structural behavior.

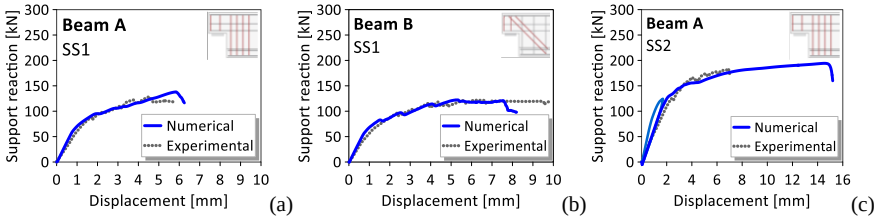


Fig. 6. Comparison between experimental and numerical responses of beam A and beam B in static schemes 1 (SS1) and 2 (SS2).

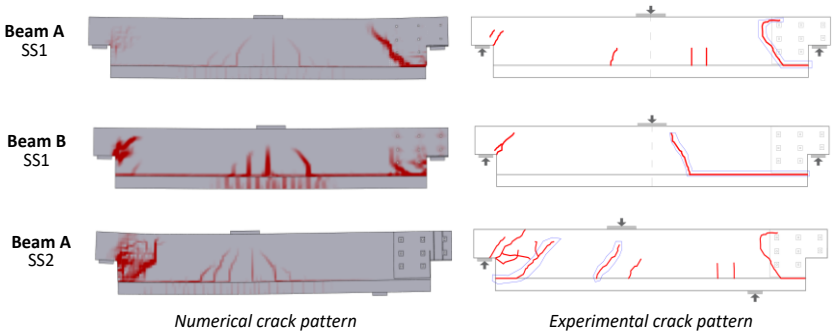


Fig. 7. Comparison between experimental and numerical crack patterns of beams A and B in static schemes 1 (SS1) and 2 (SS2).

The validated models demonstrated consistency with experimental results and offered a useful tool to explore retrofitting system performance under different configurations of those tested experimentally.

3.3 Additional numerical simulations

Further numerical investigations were performed to assess the actual response of the retrofitted half-joints and make relevant comparisons. Specifically, the structural behavior of the two specimens (Beam A and B), was analyzed under three configurations in static scheme 2:

- Undamaged half-joint designed using the S&T method;
- Damaged half-joint;
- Retrofitted-damaged half-joint with the steel jacketing system.

Numerical simulations adopted the same mechanical properties and reinforcement diameters used during the experimental campaign to be consistent with the already validated models. Fig.8 shows a comparison of the behavior of beam A and beam B under these configurations.

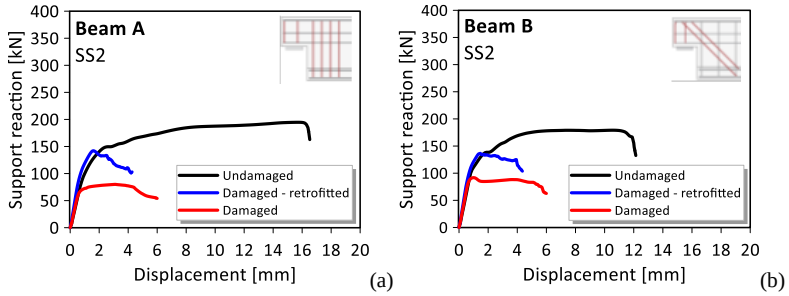


Fig. 8. Numerical responses of dapped-end beams in three different configurations in static scheme 2 (SS2): (a) Beam A; (b) Beam B.

Results indicate that the numerical models predict higher ultimate load-bearing capacities for both undamaged and damaged half-joints than the one predicted with the S&T method. In particular, the numerical predictions of the ultimate load for the undamaged dapped-end beams (A and B) are 30% and 12.5% higher, respectively, compared to the S&T estimations. For the damaged dapped-end beams, the numerical failure loads exceed the S&T predictions by 23% for beam A and 28.5% for beam B. This was because Strut-and-Tie models tend to underestimate the ultimate load, ensuring a conservative and safety-oriented solution.
Despite significantly enhancing the strength of the damaged half-joint, the steel jacketing system does not fully restore the load-bearing capacity to match that of the undamaged half-joint. The table below summarizes the failure loads across the analyzed configurations.

Table 1. Comparison of the ultimate load determined experimentally, numerically, and using the S&T method across three configurations of the dapped-end beams in SS2.

		Failure load [kN]			
	Half-joint configuration	Experimental	Numerical	S&T	Difference between numerical and S&T [%]
Beam A	Undamaged half-joint	180	195	150	30%
	Damaged half-joint	-	80	65	23%
	Retrofitted damaged half-joint	120	140	-	-
Beam B	Undamaged half-joint	-	180	160	12.5%
	Damaged half-joint	-	90	70	28.5%
	Retrofitted damaged half-joint	120	130	-	-

Failure in the retrofitted saddle occurs due to a block tearing mechanism, while the unreinforced damaged beam fails through localized cracks near the saddle notch without propagating through the entire web, as shown in Fig. 9.

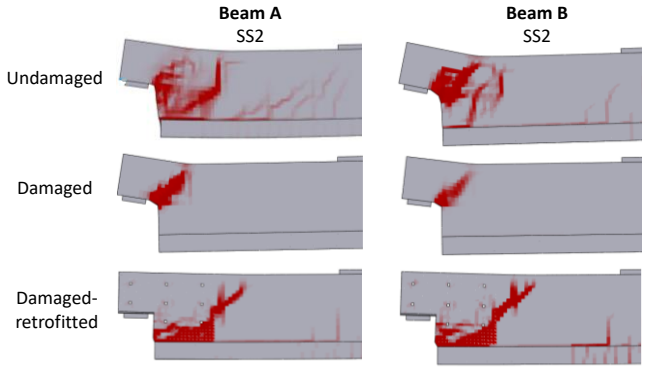


Fig. 9. Numerical crack patterns of the dapped-end beams (beam A and beam B) in three different configurations in static scheme 2 (SS2).

4 Proposal for an alternative retrofitting system

The experimental campaign and numerical simulations highlighted the main limit of the original retrofitting system: the stress concentration at the web-slab interface, involving a block tearing failure mechanism. Given this, an alternative version of the retrofitting system was proposed. The latter involves a rigid connection of the steel reinforcement to the slab, using bolts anchored into the slab with a chemical method (Fig.10a). It seeks to secure a non-invasive installation and improve overall performance with less traffic disruption of roadway operations. The anchors were designed based on the ultimate limit load (V_d) of 200 kN, evaluating the shear force (T_d) acting on the bolts. The latter was computed based on the equilibrium of the damaged retrofitted half-joint, as reported in Fig. 10b, and expressed as follows:

$$V_d \cdot \left(l_R - \frac{l_S}{2} \right) = T_D \cdot \left(0.8 \cdot h_R \right) \tag{2}$$

The shear resistance of the bolts was evaluated considering the instructions provided by the anchor manufacturers. Using M20 class 8.8 bolts, the design required four anchors per reinforcement plate, with an anchorage length of 11 cm.

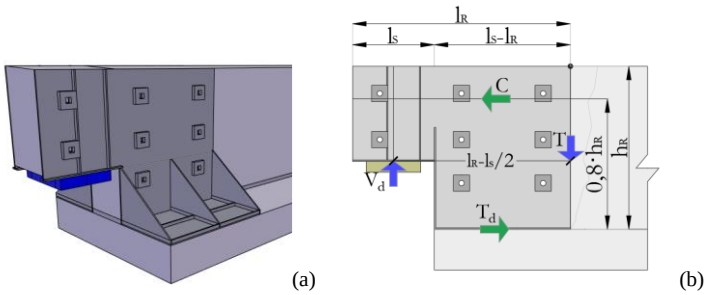


Fig. 10. Alternative retrofitting system: (a) Three-dimensional view of the modified retrofitting system, (b) Scheme for the calculation of the shear force T_d acting on the bolts for a given load V_d.

The proposed reinforcement's performances were assessed through numerical simulations under static scheme 2 and compared with various configurations for beams A and B, including damaged and undamaged half-joints (see Fig.11).

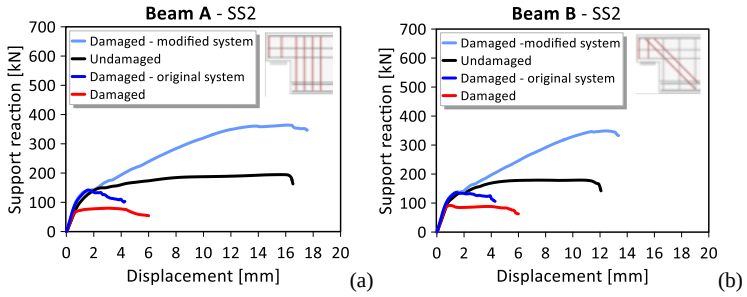


Fig. 11. Comparison of the numerical responses of dapped-end beams under various configurations, including the modified retrofitting system, in static scheme 2 (SS2): (a) Beam A; (b) Beam B.

Load-displacement curves demonstrate that the proposed reinforcement significantly increased the failure load of damaged half-joints, exceeding the resistance of the undamaged ones. The modified retrofitting system, involving chemical anchoring, achieved a load capacity of 350 kN, while the original reinforcement showed a resistance of 120 kN. Fig. 12 illustrates the crack pattern propagation in the two retrofitting systems for beam A and beam B.

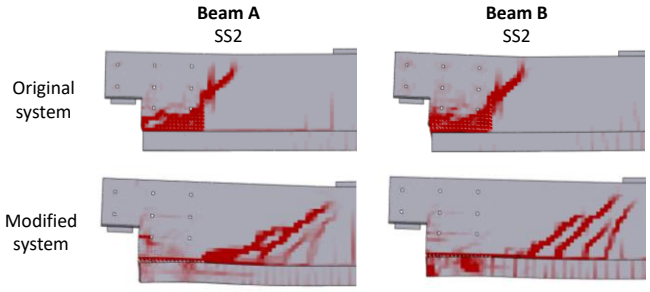


Fig. 12. Comparison of the numerical crack patterns of dapped-end beams (Beam A and B) with the original and modified retrofitting systems under static scheme 2 (SS2).

The alternative retrofitting systems effectively move the failure mechanism from the damaged region to the undamaged one, causing the translation of crack propagation from the web-slab interface to the beam's midspan. Overall, anchorage systems avoid block tearing failures, ensuring not only better distribution of the applied load but also increased capacity and ductility. These advances showcase what can be achieved using chemical anchoring and fully connected slabs to improve structural response for retrofitted-damaged dapped-end beams.

5 Conclusions

This study provided insights into the structural behavior of corrosion-damaged dapped-end beams, through a combined experimental-numerical approach. The refined numerical models developed on the STKO software platform for OpenSees showed good agreement with the experimental campaign results and allowed the generation of additional tests complementing the experimental program. The models resulted in higher load-bearing capacities for the undamaged and damaged half-joints compared to the value estimated with the S&T method. On the other hand, the steel jacketing system, though increasing the capacity of the damaged half-joint, was not able to fully recover the original load-bearing capacity and ductility, thus requiring further optimization. For this purpose, a modified retrofitting system incorporating anchoring connections to the slab was proposed. Numerical simulation results indicated that the alternative system considerably improved the retrofitted half-joint performance and shifted failure modes from the web-slab interface to the beam's midspan, away from the damaged zone. The proposed modified system shows great potential in mitigating block tearing failure mechanisms, improving load distribution, and enhancing overall structural performance while preserving the original system's primary objective of minimizing disruption to roadway traffic. These results emphasize how experimental data combined with advanced numerical modeling allow obtaining better insight into the behavior of retrofitted-damaged dapped-end beams, ensuring the safety and durability of existing infrastructure.

Acknowledgements

This paper has been part of the project PNRR-NGEU, which has received funding from the MUR - DM 351/2022.

References

1. Neves L.C., Frangopol D.M. (2005) Condition, safety and cost profiles for deteriorating structures with emphasis on bridges. *Reliability Engineering & System Safety* 89(2):185–198.
2. Lee D.J. (2015) *Bridge Bearings and Expansion Joints* (2nd edn). CRC Press.
3. Di Prisco M., Colombo M., Martinelli P., Coronelli D. (2018) The technical causes of the collapse of Annone overpass on SS.36. *Italian Concrete Days*, aicap and CTE.
4. Desnerck P., Lees J.M., Morley C.T. (2018) Strut-and-tie models for deteriorated reinforced concrete half-joints. *Engineering Structures* 161:41–54.
5. Di Carlo F., Meda A., Molaioni F., Rinaldi Z. (2023) Experimental evaluation of the corrosion influence on the structural response of Gerber half-joints. *Engineering Structures* 285:116052.
6. Rosso M.M., Asso R., Aloisio A., Di Benedetto M., Cucuzza R., Greco R. (2022) Corrosion effects on the capacity and ductility of concrete half-joint bridges. *Construction and Building Materials* 360:129555.
7. Spinella N., Messina D. (2023) Load-bearing capacity of Gerber saddles in existing bridge girders by different levels of numerical analysis. *Structural Concrete* 24:211–226.
8. Mata-Falcón J., Pallarés L., Miguel P.F. (2019) Proposal and experimental validation of simplified strut-and-tie models on dapped-end beams. *Engineering Structures* 183:594–609.
9. Belletti B., Calcavecchia B., Ferretti D., Ravasini S. (2024) Capacity assessment of uncorroded and corroded dapped-end beams by NLFE and strut-and-tie based methods. *Structural Concrete* 25(2):1275–1304.
10. Spinella N., Messina D. (2023) Load-bearing capacity of Gerber saddles in existing bridge girders by different levels of numerical analysis. *Structural Concrete* 24(1):211–226.
11. Taher F. (2005) Strengthening of critically designed girders with dapped ends. *Struct. Build.* 158:141–152.
12. Huang P.-C., Nanni A. (2006) Dapped-End Strengthening of Full-Scale Prestressed Double Tee Beam with FRP Composite. *Adv. Struct. Eng.* 9:293–308.
13. Nagy-György T., Sas G., Dăescu A.C., Barros J.A.O., Stoian V. (2012) Experimental and numerical assessment of the effectiveness of FRP-based strengthening configurations for dapped-end RC beams. *Engineering Structures* 44:291–303.
14. Quadri A.I. (2023) Behavior of disturbed region of RC precast beams upgraded with near surface mounted CFRP fiber. *Asian J. Civ. Eng.* 24:1859–1873.
15. Atta A., Taman M. (2016) Innovative method for strengthening dapped-end beams using an external prestressing technique. *Mater. Struct.* 49:3005–3019.
16. Baraghith A.T., Khalil A.H.A., Etman E.E., Behiry R.N. (2023) Improving the shear behavior of RC dapped-end beams using precast strain-hardening cementitious composite (P-SHCC) plates. *Structures* 50:978–997.

17. Bertagnoli G., Ferrara M., Giordano L., Malavisi M. (2023) Preliminary Investigation on Steel Jacketing Retrofitting of Concrete Bridges Half-Joints. *Applied Sciences* 13(14):8181.
18. McKenna F., Fenves G.L., Scott M.H. (2000) Open system for earthquake engineering simulation. University of California, Berkeley, CA.
19. Petracca M., Candeloro F., Camata G. (2017) *ASDEA Software STKO user manual.*
20. Petracca M., Pelà L., Rossi R., Zaghi S., Camata G., Spacone E. (2017) Microscale continuous and discrete numerical models for nonlinear analysis of masonry shear walls. *Construction and Building Materials* 149:296–314.
21. Di Trapani F., Villar S., Di Benedetto M., Petracca M., Camata G. (2024) Seismic response of unreinforced masonry building aggregates: Investigation on the "aggregate-effect" based on an elementary building aggregate. *Engineering Structures* 316:118301.
22. Oliver J., Huespe A.E., Cante J.C. (2008) An implicit/explicit integration scheme to increase computability of non-linear material and contact/friction problems. *Comput. Methods Appl. Mech. Engrg.* 197:1865–1889.
23. Di Trapani F., Di Benedetto M., Petracca M., Camata G. (2024) Local infill-frame interaction under seismic loads: Investigation through refined micro-modeling. *Engineering Structures* 315:118088.